journal

J. Am. Ceram. Soc., 79 [2] 461-69 (1996)

In Situ Toughened Silicon Carbide with Al-B-C Additions

Joe J. Cao,* Warren J. MoberlyChan, Lutgard C. De Jonghe,* Christopher J. Gilbert,* and Robert O. Ritchie

Center for Advanced Materials, Materials Sciences Division, Lawrence Berkeley National Laboratory, and Department of Materials Science and Mineral Engineering, University of California, Berkeley, CA 94720-1760

"*In situ* toughened" silicon carbides, containing Al, B, and C additives, were prepared by hot pressing. Densification, phase transformations, and microstructural development were described. The microstructures, secondary phases, and grain boundaries were characterized using a range of analytical techniques including TEM, SEM, AES, and XRD. The modulus of rupture was determined from four-point bend tests, while the fracture toughness was derived either from bend tests of beam-shaped samples with a controlled surface flaw, or from standard disk-shaped compact-tension specimens precracked in cyclic fatigue. The *R*-curve behavior of an *in situ* toughened SiC was also examined. A steady-state toughness over 9 MPa·m$^{1/2}$ was recorded for the silicon carbide prepared with minimal additives under optimum processing conditions. This increase in fracture toughness, more than a factor of three compared to that of a commercial SiC, was achieved while maintaining a bend strength of 650 MPa. The mechanical properties were found to be related to a microstructure in which platelike grain development had been promoted and where crack bridging by intact grains was a principal source of toughening.

I. Introduction

THE advantages of silicon carbide in high-temperature structural applications include high strength, creep resistance, and chemical stability. A disadvantage, however, has been its low fracture toughness, typically of 2 to 4 MPa·m$^{1/2}$. A number of attempts have recently been made to improve the fracture toughness of this ceramic, with toughness values reported as high as 6 to 8 MPa·m$^{1/2}$. These efforts include toughening by heterophase dispersion,[1,2] by incorporation of coated α-SiC platelets in a β-SiC matrix,[3-5] and by addition of Al_2O_3[6-8] or Al_2O_3–Y_2O_3.[9-12] The aims of the latter efforts were to achieve a platelike microstructure in which grain bridging and crack deflection were promoted by the presence of substantive amounts of the additives.[6-8,10-12] This provided an *in situ* toughened material with a microstructure akin to that of tough silicon nitride. Suzuki,[6] using alumina as an additive, and later Mulla and Krstic,[7] produced a microstructure consisting of elongated α-SiC grains. Their materials showed a modulus of rupture (MOR) of about 600 MPa and a fracture toughness of 5 to 6 MPa·m$^{1/2}$ determined by the single-edge notched-beam method (with no precracking). Silicon carbides with alumina–yttria additives were prepared by Lee and Kim[10] and more recently by Padture and Lawn.[11,12] These materials, containing 10 to 26 wt% YAG, were reported to exhibit fracture toughness of ~8 MPa·m$^{1/2}$, as determined by the Vickers indentation method.[10,11]

The objective of the present work was to augment the toughening of SiC using aluminum metal, boron, and carbon in relatively low concentrations as sintering aids. This combination of additives, under processing conditions described here, favorably affected the microstructure and phase transformation characteristics and yielded a silicon carbide with a steady-state fracture toughness in excess of 9 MPa·m$^{1/2}$, while at the same time retaining a high modulus of rupture. The mechanical properties, evaluated at room temperature, and the related microstructural characteristics were compared to those of a baseline commercial SiC ceramic (Hexoloy SA).

II. Experimental Procedure

Submicrometer β-SiC (BSC-21, Ferro, Cleveland, OH), with a mean particle size of 0.15 μm, was mixed with Al, B, and C additives in toluene. The Al metal (H-3, Valimet, Stockton, CA), which had an average particle size of 3 μm, constituted from 1 to 6 wt% of the powder. For all mixtures prepared, the boron (Callery Chemical, Callery, PA) content was kept at 0.6 wt%. The carbon was introduced as 4 wt% Apiezon wax (Biddle Instruments, Plymouth Meeting, PA), which was converted upon pyrolysis to yield ~2 wt% C.

The slurries of SiC powder with additives were ultrasonically agitated for 5 min and passed through a 325 mesh sieve. Following stir-drying, the mixture was reground in a mortar and pestle and screened through a 200 mesh sieve. After cold die compression at 35 MPa, the green compacts were hot-pressed in graphite dies lined with graphite foil, at temperatures between 1700° and 1950°C, for 15 min to 4 h, at 50 MPa, under flowing argon. Three disks, 38 mm in diameter and 4 mm thick, were fabricated during each processing run, using graphite spacers between specimens.

Densities of the hot-pressed specimens were determined by Archimedes' method. Optical, X-ray, and electron beam methods were used for the microstructural and chemical characterization. These methods included optical microscopy (OM), X-ray diffraction (XRD), scanning electron microscopy (SEM), and conventional and high-resolution transmission electron microscopy (TEM and HR-TEM). Compositional information was obtained from energy-dispersive spectroscopy (EDS), wavelength-dispersive X-ray analysis (WDS), parallel electron energy loss spectroscopy (PEELS), and Auger electron spectroscopy (AES).

The basic mechanical properties of the silicon carbides were evaluated on beams of 2.7 by 3 by 30 mm sectioned from the hot-pressed billets. The beams were tested in a four-point bending jig with an outer span of 25.4 mm, an inner span of 9.5 mm, and at a crosshead speed of 0.05 mm/min. The tensile surfaces of the specmens were polished to a ~1 μm diamond finish, and the tensile edges were beveled to reduce edge flaws. For fracture toughness measurements, a controlled surface flaw was introduced on the tensile surface with a Knoop indenter, using a load between 98 and 137 N. Upon bending, the indentation crack experiences a total stress intensity K_t, which is the sum of the residual stress intensity K_r and the applied stress intensity K_a,[13-15] i.e.,

R. H. Dauskardt—contributing editor

Manuscript No. 192749. Received March 21, 1995; approved August 28, 1995.
Supported by the Director, Office of Energy Research, Office of Basic Energy Sciences, Materials Sciences Division of the U.S. Department of Energy, under Contract No. DE-AC03-76SF00098.
*Member, American Ceramic Society.

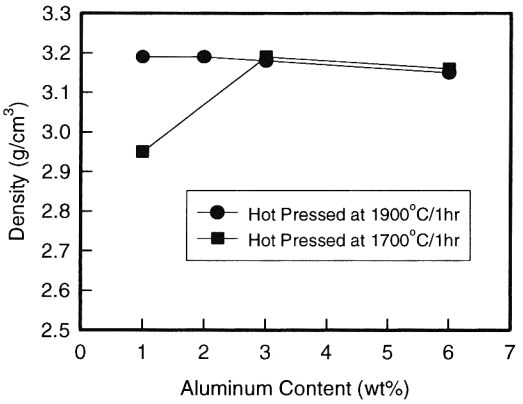

Fig. 1. Densities of silicon carbides hot pressed at 1700°C and 1900°C with various amounts of Al, together with 0.6 wt% B and 2 wt% C additives.

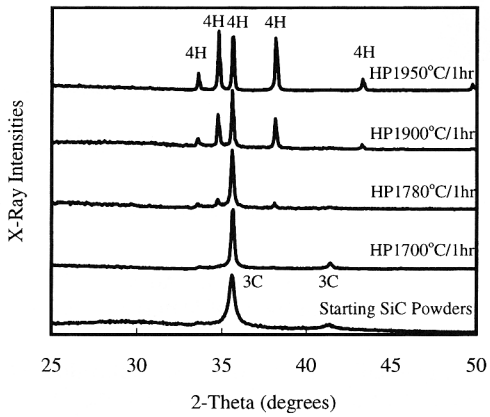

Fig. 2. X-ray diffraction spectra of the starting β-SiC powder and of silicon carbides hot-pressed at various temperatures with 3wt%Al–0.6wt%B–2wt%C additives.

$$K_t = K_r + K_a \tag{1}$$

The residual stress intensity K_r has a simple form:[13–15]

$$K_r = \xi(E/H)^{1/2} P/a^{3/2} \tag{2}$$

where E and H are the elastic modulus and hardness of the material, P is the indentation load, a is the crack size, and ξ is a dimensionless constant dependent only on the indenter geometry.

For a semicircular surface crack, the applied stress intensity was calculated from the relation[16,17]

$$K_a = \frac{2}{\sqrt{\pi}} \sigma_a \sqrt{a} \tag{3}$$

where σ_a is the applied stress. The total stress intensity is therefore

$$K_t = \xi(E/H)^{1/2} P/a^{3/2} + \frac{2}{\sqrt{\pi}} \sigma_a \sqrt{a} \tag{4}$$

Setting $K_t = K_c$ for equilibrium crack extension, Eq. (4) can be rearranged:

$$\sigma_a = \frac{\sqrt{\pi}}{2\sqrt{a}} [K_c - \xi(E/H)^{1/2} P/a^{3/2}] \tag{5}$$

The failure condition (instability) is defined by the maximum in the applied stress, σ_a, when $d\sigma_a/da = 0$. Thus we have

$$a_m = [4\xi(E/H)^{1/2} P/K_c]^{2/3} \tag{6}$$

$$\sigma_m = \frac{3\sqrt{\pi}}{8} K_c \left[\frac{K_c}{4\xi(E/H)^{1/2} P}\right]^{1/3} \tag{7}$$

When Eqs. (6) and (7) are combined, the fracture toughness is calculated as follows:

$$K_c = \frac{8}{3\sqrt{\pi}} \sigma_m \sqrt{a_m} \tag{8}$$

where σ_m is the fracture strength of the indented beams and a_m is the crack size at instability (see Fig. 7). For each processing condition, four beams were used to measure the average fracture toughness K_c, and at least five beams were tested to determine modulus of rupture (MOR).

The fracture toughness and resistance curve (R-curve) behavior of an optimized silicon carbide was also evaluated using an ASTM E399 standard disk-shaped compact-tension DC(T) specimen of width $W = 28.6$ mm and thickness $B = 3.26$ mm. Prior to data collection, the specimen was precracked under cyclic loading.† Crack lengths were continuously monitored using a combination of several methods, including electrical-potential measurements across a thin (~100 nm) NiCr film evaporated onto the specimen surface, compliance measurements using a 350 Ω strain gauge attached to the back face of the specimen, and direct size measurement with a high-resolution optical traveling microscope. Details of these experimental techniques have been reported elsewhere.[18] Before measuring the resistance curve, the specimen was cycled for ~24 h at a sufficiently low ΔK such that no crack growth was detected over this interval. This precaution minimized the effect on the measured initiation toughness K_0 of any preexisting damage and crack-tip shielding.‡ Subsequently, the resistance curve was measured by bringing the specimen to failure under load control at a rate of ~0.05 MPa·m$^{1/2}$/s.

III. Results and Discussion

(1) Processing and Microstructural Development

The densitites of the silicon carbides, hot-pressed at 1700° and at 1900°C, respectively, have been plotted versus the added content of metallic aluminum in Fig. 1. The combination of Al,

†The fatigue precrack was made under cyclic loading at 25 Hz with a sinusoidal wave form on a computer-controlled servo-hydraulic testing machine several millimeters beyond the wedge-shaped starter notch at an applied stress intensity range of $\Delta K = 7$ MPa·m$^{1/2}$, with load ratio $R = K_{min}/K_{max} = 0.1$.

‡In grain-bridging ceramics, frictional wear in the interfaces between interlocking grains that span the crack during cyclic fatigue loading can lead to an almost complete degradation of crack bridging in the crack wake. See Refs. 19 and 20.

Table I. Processing Conditions and SiC Polytypes

Material	Starting powder*	Sintering aids	Hot-press conditions	SiC polytypes†
B1	100(3C)	3Al–0.6B–2C	1700°C/1 h	100(3C), <1(4H)
B2	100(3C)	3Al–0.6B–2C	1780°C/1 h	80(3C), 20(4H)
B3	100(3C)	3Al–0.6B–2C	1900°C/1 h	25(3C), 75(4H)
B4	100(3C)	3Al–0.6B–2C	1900°C/4 h	100(4H)
B5	100(3C)	3Al–0.6B–2C	1950°C/1 h	100(4H)
A1	99.5(3C), 0.5(6H)	3Al–0.6B–2C	1900°C/15 min	30(3C), 40 (4H), 30(6H)

*Weight percentages of the starting powder of each SiC polytypes as indicated in parentheses. †Volume percentage calculated based on XRD using the method by Ruska *et al.*[21]

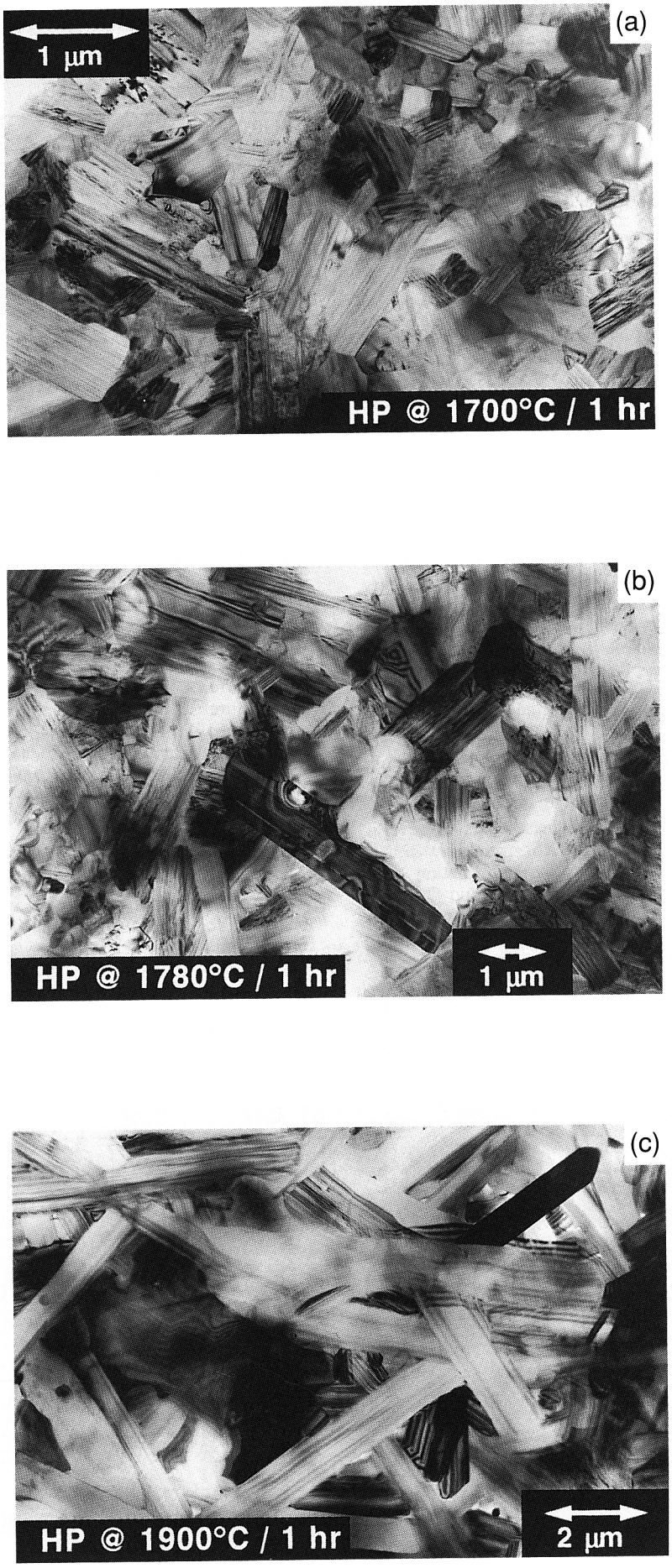

Fig. 3. TEM micrographs of silicon carbides hot-pressed at various temperatures with 3wt%Al–0.6wt%B–2wt%C additives: (a) 1700°C, (b) 1780°C, and (c) 1900°C.

Table II. Processing Conditions, Microstructural Results, and Mechanical Properties of Hot-Pressed Silicon Carbides with 3wt%Al–0.6wt%B–2wt%C Additions

Material	Hot-press Conditions	Density (g/cm^3)	SiC Grain size†			MOR (MPa)	K_c^* ($MPam^{1/2}$)
			Length (μm)	Width (μm)	Aspect ratio		
B1	1700°C/1 h	3.19	1.0 (0.5)	0.4 (0.2)	2.8 (0.9)	600 (90)	4.3 (0.1)
B2	1780°C/1 h	3.19	2.7 (0.9)	0.7 (0.3)	4.0 (1.4)	650 (70)	5.9 (0.3)
B3	1900°C/1 h	3.18	5.5 (2.4)	0.7 (0.2)	7.6 (2.3)	660 (20)	9.1 (0.5)
B4	1900°C/4 h	3,18	8.9 (2.9)	1.0 (0.3)	9.0 (2.9)	650 (20)	9.5 (0.6)
B5	1950°C/1 h	3,18	13.3 (3.6)	2.6 (0.9)	5.4 (1.6)	540 (50)	8.0 (0.3)
Hexoloy‡	N/A§	3.14	~5	~5	~1	400 (40)	2.8 (0.2)

*K_c was measured using the controlled surface flaw method in four-point bending. †Data in the parentheses indicate standard deviation. ‡Commercial SiC (Hexoloy SA) from Carborundum, Niagara Falls, NY. §Sintering temperature has not been reported.

B, and C as sintering additives has evidently been effective for densification. When silicon carbide was hot-pressed at 1700°C, 3 wt% Al was sufficient to reach nearly full density, whereas at 1900°C, only 1 wt% Al was needed. The effectiveness of Al as a sintering aid for SiC has been evidenced, for example, in the previous work of De Jonghe *et al.*[3–5] in which β-SiC, containing up to ~32 vol% of oxide-coated α-SiC platelets, was hot-pressed to nearly full density at temperatures below 1700°C.

X-ray diffraction spectra from the polished surfaces of the hot-pressed SiC with 3wt%Al–0.6wt%B–2wt%C additions and processed at different temperatures are shown in Fig. 2, together with the spectrum of the β-SiC starting powder. After processing at 1700°C, the SiC remained mainly as the β-phase (3C); the peak broadness, however, was significantly reduced from that of the original powders, indicating that the β-phase grains had grown. The β-to-α phase transformation was essentially complete after hot-pressing at 1950°C: the relative XRD intensities of this specimen had a near-perfect match with those of a 4H-SiC standard,[21] indicating at the same time that the 4H grains were randomly distributed. No other SiC polytypes (e.g., 6H or 15R) were evident at any temperature. Favored formation of the 4H polytype in Al-containing SiC had been reported by Hamminger *et al.*[22] when studying the structures of several pressureless-sintered SiC compositions. Shinozaki *et al.*[23–25] also found that the 3C-to-4H phase transformation was enhanced by the presence of Al together with B and C. However, Shinozaki *et al.* reported that the 3C-SiC transformed to 4H-SiC through an intermediate structure of 15R, which was not observed in the present study (neither by XRD nor by TEM). The differences in crystal structures of the transformation products were believed to originate in the differences in the starting β-SiC powders. Pure crystalline β-phase powders were used here, while Shinozaki *et al.*[23–25] used powders containing 29% of a "disordered" phase. A β-SiC seeded with 0.5 wt% of submicrometer 6H-SiC hot-pressed at 1900°C for 15 min formed 30% of 6H, 40% of 4H, with 3C as the balance (see Table I). The minimal addition of 6H seeds caused substantial 3C to 6H transformation or, more appropriately, the growth of the 6H grains. A direct transformation of the 3C to 4H has also been reported with Y_2O_3–Al_2O_3 additives.[10]

When only B and C were used as additives, the β-to-α phase transformation began at temperatures greater than 1950°C.[26–28] The addition of a small amount of metallic aluminum or aluminum compounds lowered this phase transformation temperature. Onset of the β-to-α phase transformation has been reported at approximately 1800°C with 1.5wt%Al–1.2wt%B–4wt%C additions.[24,25] In the present study, 3 wt% of metallic Al with 0.6 wt% B and 2 wt% C was found to strongly promote the β-to-α phase transformation by further lowering the onset temperature. A trace of 4H-SiC was detected at a hot-pressing temperature as low as 1700°C by both XRD and TEM. Hot-pressing at 1780°C for 1 h caused 20% 3C to 4H transformation (Table I), as determined using the method of Ruska *et al.*[21] After hot-pressing at 1900°C for 1 h, 75% 4H formed, and at 1950°C the transformation was complete.

Figures 3(a) through 3(c) show TEM images of microstructures of SiC hot-pressed with 3wt%Al–0.6wt%B–2wt%C at 1700°, 1780°, and 1900°C, respectively. As the sintering temperature increased, the SiC grains grew into platelike shapes. Cross-sectional grain length, grain width, and aspect ratios were measured for at least 50 grains in TEM images or in SEM micrographs of etched surfaces, and the results are listed in Table II. For platelike grains, the aspect ratios determined from two-dimensional measurements tend to underestimate the true aspect ratios in three dimensions. It was also noted that numerous small grains (<0.2 μm) were observed in the microstructures for silicon carbides processed at 1700° and 1780°C.

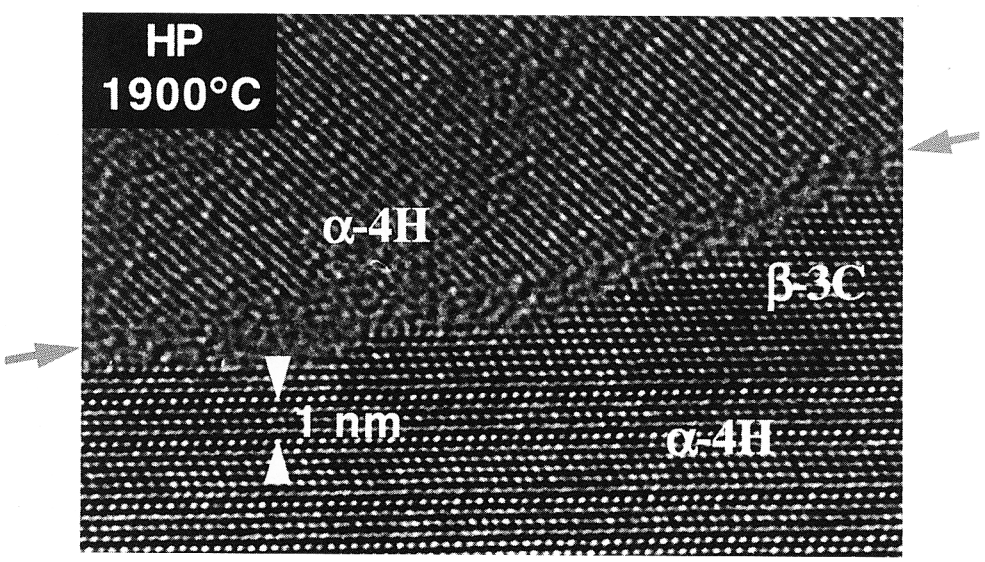

Fig. 4. High-resolution TEM micrograph shows lattice image of two neighboring grains in specimen B3, indicating an amorphous grain boundary phase of less than 1 nm thick.

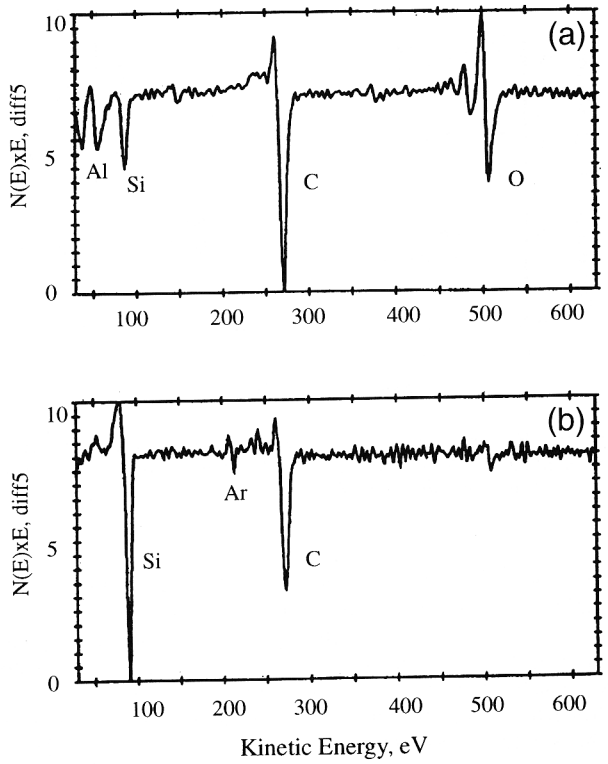

Fig. 5. Auger electron spectrum acquired of (a) an intergranular fracture surface and (b) of the same area after ion-sputtering less than 1 nm of material from the surface.

Because these small grains were believed not to contribute to toughening, they were not included in the measurements reported in Table II.

The growth of platelike grains was found to be associated with the 3C-to-4H phase transformation. The silicon carbide hot-pressed at 1700°C showed a duplex grain structure with approximately two-thirds of the material being β-phase grains of about 1 μm in length by 0.5 μm in width, while the other one-third of the material consisted of β grains, an order of magnitude smaller in size. A few large grains in this SiC had larger aspect ratios, and electron diffraction determined these grains to be of a dual structure (i.e., partially 3C and partially 4H). When processed at 1780°C, the majority of the grains had platelike shapes and showed the dual grain structures. At 1900°C, the grains had grown longer, and the portion of the 4H-phase increased. After hot-pressing at 1950°C, the grains were larger both in length and in width and exhibited only the 4H-phase.

Secondary phase regions, having similar sizes as the added Al powders, were observed on SEM micrographs of polished surfaces. Energy-dispersive and wavelength-dispersive X-ray spectroscopy (EDS and WDS) showed that these secondary phase regions contained Al and were free of Si. AES further determined that major secondary phases were aluminum-boron carbides, while other phases such as aluminum oxycarbides, aluminum oxides, and aluminum carbides were occasionally detected. Electron diffraction and lattice imaging by TEM have confirmed the existence of these secondary phases.[4] Graphite inclusions, often reported in SiC with B and C additions,[24,29] were not observed.

The formation of secondary phases was attributed to the sintering additives present in concentrations well above their solubilities in SiC. The solubility limit reported for aluminum in SiC is 0.26 and 0.50 wt% at 1800° and 2000°C, respectively, and for boron it is 0.1 wt% at 2500°C.[30] Thus, secondary phases should be expected to form, especially as the Al melts well below the processing temperatures. In the presence of the added aluminum, carbon, and boron, together with oxygen from the

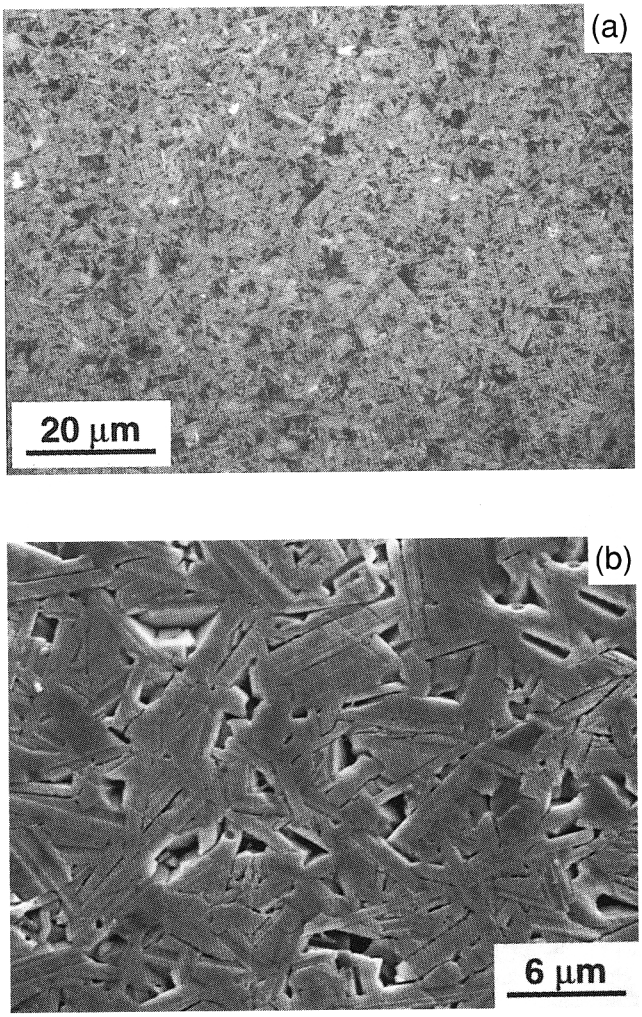

Fig. 6. (a) Optical and (b) SEM micrographs of an etched surface of specimen B3, showing elongated SiC grains.

powder surfaces, several phases are thermodynamically possible. Examples are $Al_8B_4C_7$, which has a melting point near 1800°C,[31] and Al_4O_4C, which has an eutectic reaction with Al_2O_3 at 1840°C.[32] Ternary and quaternary phase diagrams among elements of Si, Al, B, C, and O have been shown elsewhere.[4]

The possible presence of liquid phases at grain boundaries was expected to play a major role in densification and grain growth. A high-resolution lattice image of two neighboring

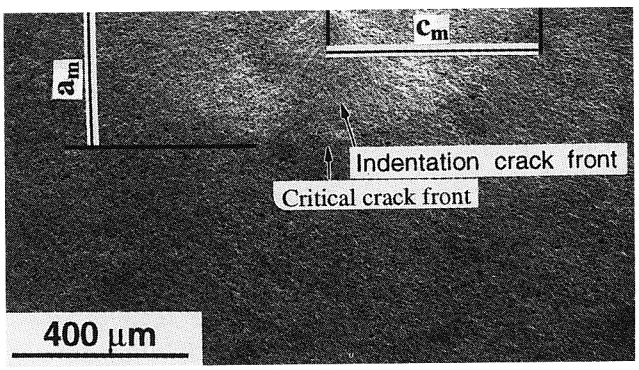

Fig. 7. SEM micrograph of a precrack induced by the Knoop indentation. During bending, the crack propagated in a stable manner, and the critical crack front became elliptical. The depth "a_m" of the crack at instability was used to calculate fracture toughness in Eq. (8).

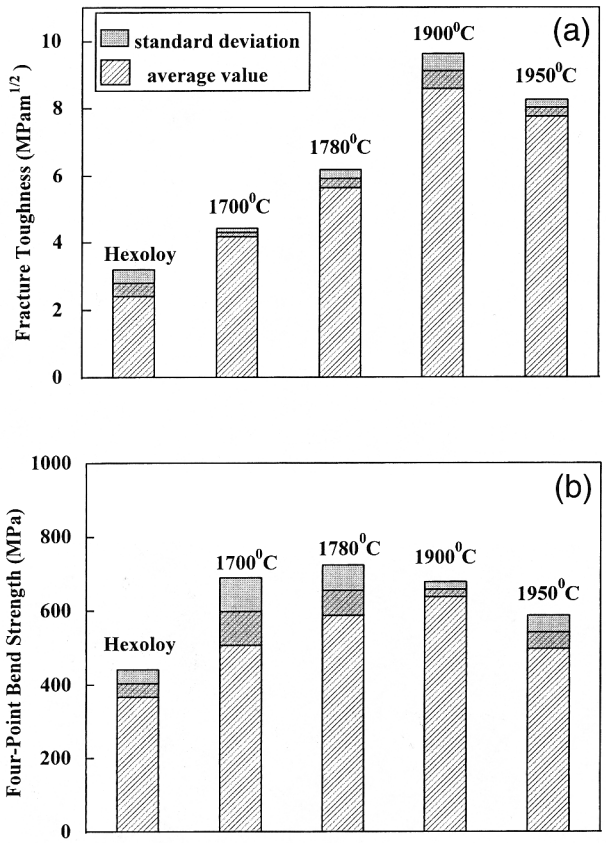

Fig. 8. (a) Fracture toughness (measured from bend tests with a controlled surface flaw) and (b) four-point bend strength of silicon carbides hot-pressed between 1700° and 1950°C with 3wt%Al–6wt%B–2wt%C additions. Measured data for Hexoloy SiC are included for comparison.

grains in specimen B3 is shown in Fig. 4, revealing an amorphous grain boundary phase less than 1 nm thick. An Auger electron spectrum, acquired from an intergranular fracture surface, showed the presence of Si, C, Al, O (Fig. 5(a)). After sputtering away less than 1 nm of material from this surface, the Al and O signals disappeared (Fig. 5(b)). The Si and C

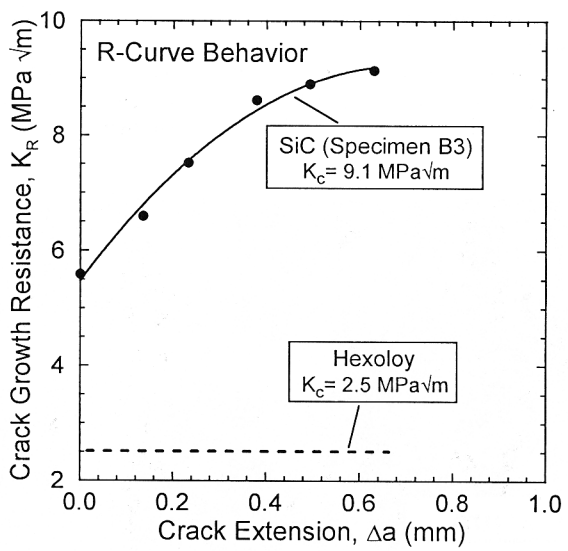

Fig. 9. A crack growth resistance curve, K_R, as a function of crack extension Δa for specimen B3, in comparison to the behavior of Hexoloy SiC. Note the very high plateau (steady-state) fracture toughness of 9.1 MPa·m$^{1/2}$.

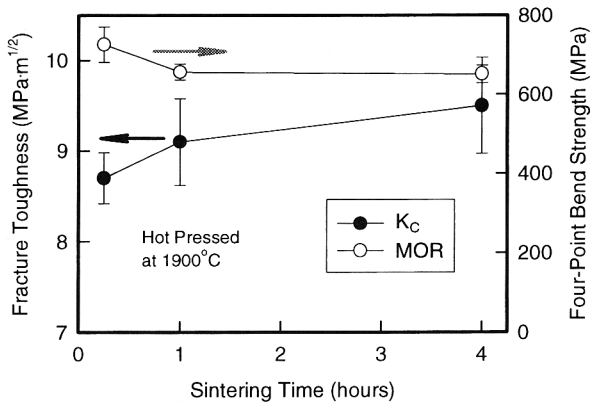

Fig. 10. Fracture toughness K_c (determined from bend tests with a controlled surface flaw) and four-point bend strength MOR as a function of hot-pressing time at 1900°C.

signals were from the bulk SiC; the O signal could be from adsorbed oxygen, since the specimen was fractured in air. It can be concluded at this point that the grain boundary phase contained Al; however, the exact chemistry of the grain boundary phase has not yet been determined with certainty.

Sintering of the present Al, B, and C-doped SiC was believed to be a liquid-phase process, similar to that for the Al_2O_3-added SiC described by Suzuki.[6] A likely scenario that could be envisioned was as follows. During heating, metal aluminum melted, and B, C, and O were presumed to transport into the aluminum melt and form secondary phases. The liquid phase(s)

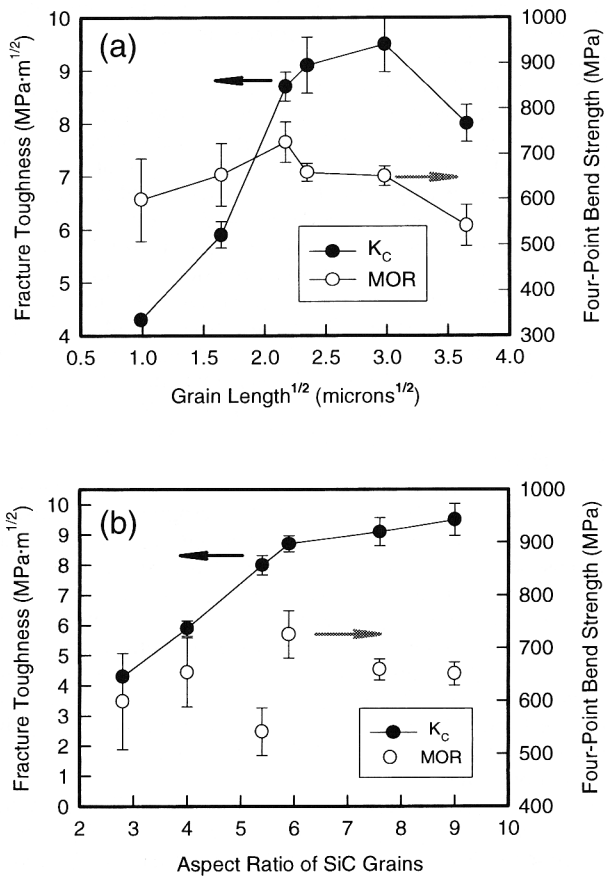

Fig. 11. Fracture toughness K_c (determined in bend tests with a controlled surface flaw) and four-point bend strength MOR (a) as a function of the square root of grain length and (b) as a function of grain aspect ratio in hot-pressed silicon carbides.

flowed, filling pores between the nearby SiC particles and engulfing many grains, as observed by TEM.[4] Meanwhile, aluminum vapor coated the SiC particle surfaces and reacted with the native oxide on the powder surface as well as the added carbon and boron to form a liquid grain boundary phase. In the presence of an applied pressure, particle rearrangement occurred. A liquid-phase sintering mechanism, i.e., a solution–reprecipitation process, caused gradual densification coupled with grain growth. At this stage, corresponding to sintering at $\leq$1700°C with 3 wt% or more Al addition, a fine-grained dense 3C-SiC was obtained. At higher sintering temperatures, SiC transformed from 3C to 4H, accompanied by the formation and growth of platelike grains with increasing aspect ratios. At temperatures above 1900°C, however, grain growth of 4H-SiC continued while the 3C phase gradually diminished, while at the same time the grain aspect ratios decreased.

An optimal microstructure, in terms of high-aspect-ratio platelike grains with grain boundary phases less than 1 nm thick, was produced by hot-pressing at 1900°C. Figure 6 shows optical and SEM micrographs of the SiC etched by boiling in Murakami's reagent (10 g of NaOH and 10 g of $K_3Fe(CN)_6$ in 100 mL H_2O) for 45 min. Platelike grains are shown here; apparent porosity in these microstructures resulted from etching damage and from the preferential removal of secondary phases.

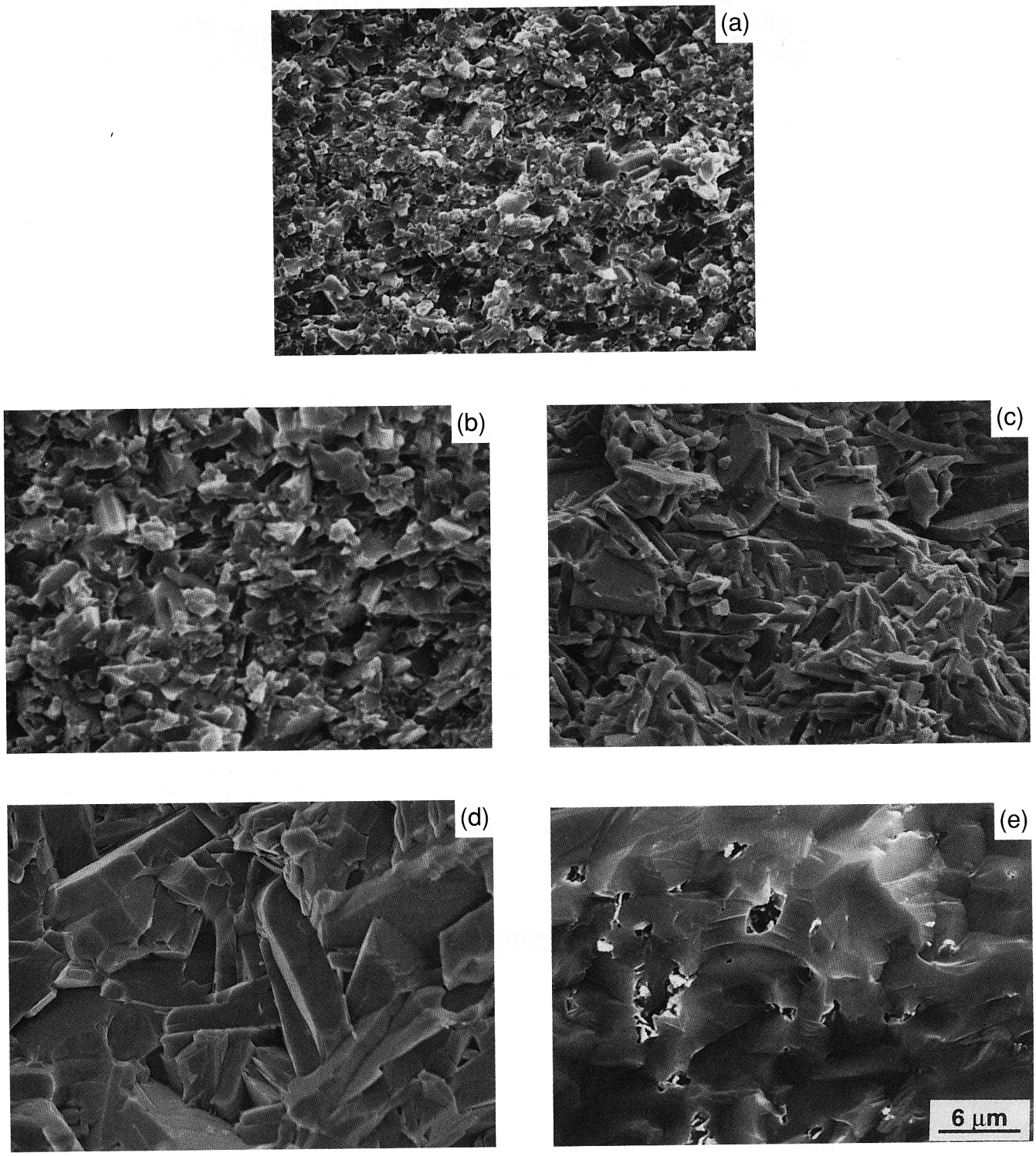

Fig. 12. SEM fractographs of silicon carbides hot-pressed at various temperatures: (a) 1700°C/1 h, (b) 1780°C/1 h, (c) 1900°C/1 h, (d) 1950°C/1 h, and (e) Hexoloy SiC.

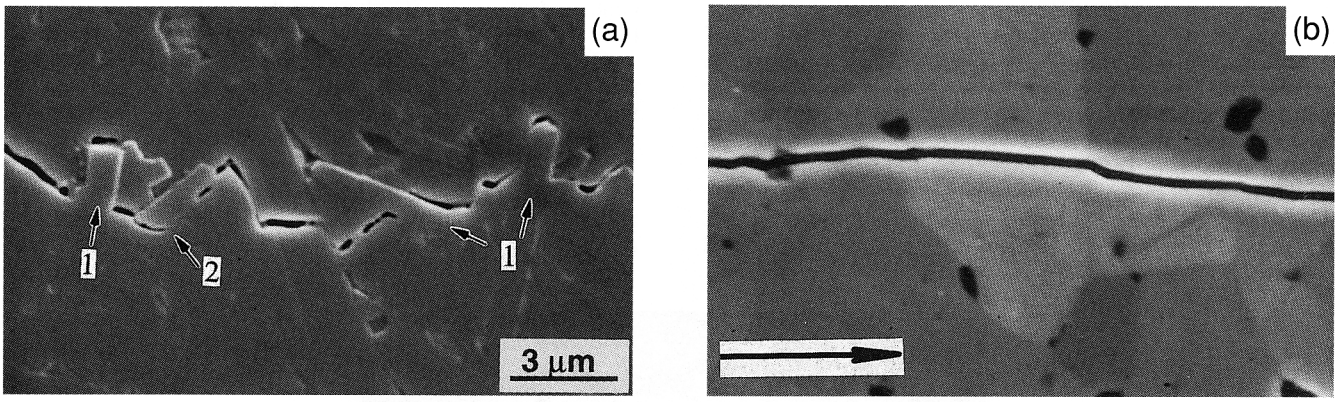

Fig. 13. SEM images of crack paths from Vickers indentation in (a) an *in situ* toughened SiC and (b) Hexoloy SiC. Note the bridged (as shown by arrow 1) and deflected (arrow 2) path in (a), versus the straight and transgranular path in (b). The horizontal arrow shows direction of crack growth.

A TEM micrograph and an Auger electron spectrum of this sample were shown in Fig. 3(c) and Fig. 5, respectively.

(2) Mechanical Properties

During bending of the indented beams, the residual stresses contribute to the fracture process, causing stable crack growth even in materials that have no *R*-curve behavior.[13,14] Figure 7 is an SEM fractograph of sample B1 showing an initial well-defined semicircular indentation crack front and a semielliptical crack front at instability. Near the top surface the crack had grown from c_0 to c_m, while in the depth direction the crack had grown from a_0 to a_m. To calculate the fracture toughness conservatively, we have taken the minor half-axis of the critical crack as the crack size in Eq. (8). Figures 8(a) and 8(b) show the fracture toughness (measured from bend tests with a controlled surface flaw) and four-point bend strength of the silicon carbides hot-pressed between 1700° and 1950°C, for 1 h, with 3wt%Al–0.6wt%B–2wt%C additions. Since fracture toughness values are sensitive to the particular testing methodology,[33] similar measurements were made on a commercial SiC (Hexology SA) for comparison. When the sintering temperature increased from 1700° to 1900°C, the fracture toughness increased from 4.3 to 9.1 MPa·m$^{1/2}$. The latter value is over 3 times as high as that of Hexology SiC. These values were consistent with more precise measurements made using fatigue precracked DC(T) specimens; the SiC hot-pressed at 1900°C for 1 h exhibited significant resistance-curve behavior (Fig. 9), rising from an initiation value of K_0 = 5.5 MPa·m$^{1/2}$ to a plateau value of K_c = 9.1 MPa·m$^{1/2}$. The maximum crack growth resistance was reached after ~600 μm of crack extension. Such behavior has been attributed to extensive crack bridging by the *in situ* grown platelike grains, as is discussed below. The fracture toughness of Hexology SiC was determined by similar methods to be 2.5 MPa·m$^{1/2}$, with no resistance-curve behavior being detected using the precracked DC(T) specimens. The measured fracture toughness values from the two techniques are clearly quite consistent.

As the hot-pressing temperature was raised from 1700° to 1900°C, the average bend strength increased slightly, and the scatter of the measured data decreased significantly (Figs. 8(a) and (b)). The standard deviation of strength was reduced from 90 MPa (~15%) to 20 MPa (~3%). Above 1900°C, however, the bend strength decreased, presumably as a result of larger preexisting flaws induced by excessive grain growth.

To examine the effect of sintering time on fracture toughness and bend strength, silicon carbides were hot-pressed and held at 1900°C for times ranging from 15 min to 4 h (Fig. 10). As the hot-pressing time increased, the fracture toughness increased, while the strength slightly decreased. These changes were believed to originate in the differences in grain size. The increasing scatter in measured toughness was mostly the result of the increasing difficulty in measuring the precrack length in the coarser microstructures.

Fracture toughnesses and bend strengths have been plotted versus the square root of grain length in Fig. 11(a). This plot indicates that some degree of grain growth was beneficial for both toughness and strength. Upon increasing the grain length from ~1 μm to ~9 μm, the fracture toughness increased by more than a factor of 2; for an increase in the grain length from ~1 to ~5 μm, some improvement in strength was also observed. From elementary fracture mechanics, it is known that strength relates to toughness and flaw size. The strength increase with grain growth was presumably the result of the much improved toughness. In Fig. 11(b) the fracture toughness and bend strength are plotted versus the aspect ratios of the platelike grains. The fracture toughness increased from 4.3 to

Table III. Processing Conditions and Properties of an *in situ* Toughened Silicon Carbide

Sintering additives	3wt%Al–0.6wt%B–2wt%C
Hot-pressing conditions	1900°C/1 h
Density	3.18 g/cm^3
Crystal structure	75% (4H) + 25% (3C)
Grain size (cross-sectional)	
Length	5.5 ± 2.4 μm
Width	0.7 ± 0.2 μm
Aspect ratio	7.6 ± 2.3
Hardness (Vickers, 500 g load)	24.0 ± 1.7 GPa
Four-point bend strength	660 ± 20 MPa
Fracture toughness	
Four-point bending with controlled-surface flaw	9.1 ± 0.4 MPa·m$^{1/2}$
DC(T) with fatigue precrack	9.1 MPa·m$^{1/2}$

9.5 MPa·m$^{1/2}$ when the aspect ratio increased from ~3 to ~9. The strength, however, was not sensitive to the aspect ratio.

Figures 12(a) through 12(d) show fractographs of silicon carbides hot-pressed at various temperatures. At relatively low sintering temperatures (1700° and 1780°C), the fracture mode was predominantly intergranular. When sintered at 1900°C, some transgranular fracture occurred; however, intergranular fracture still dominated, with the majority of the platelike grains exhibiting pullout. At 1950°C, the material (B5) showed a larger fraction of transgranular fracture, particularly for the larger grains. In comparison, the fracture surface of Hexoloy SiC exhibited complete transgranular fracture, as is evident in Fig. 12(e).

Toughening in these silicon carbides was primarily attributed to grain bridging and subsequent grain pullout. Partially debonded platelike grains, which resided just behind the crack tip, bridged the crack, thereby reducing the effective stress intensity.[34] With very fine grains (for example, after hot-pressing at 1700°C), toughening from grain bridging and pullout was minimal. After hot-pressing at higher temperatures (e.g., at 1900°C), growth of the platelike grains with increased aspect ratio highly enhanced the effect of crack bridging, resulting in a significant improvement in fracture toughness and, to a lesser extent, in strength.

Another contribution to the overall toughening was expected from crack deflection. This mechanism of toughening is known to be governed by the aspect ratio of the elongated grains,[35] which is plotted in Fig. 11(b). The crack path from a Vickers indent is shown in Fig. 13(a), where crack deflection has been marked by arrow 1 and grain pullout by arrow 2. On the other hand, the indentation crack path is quite straight in Hexoloy SiC as shown in Fig. 13(b). More detailed analysis on toughening mechanisms and studies on cyclic fatigue behavior in the *in situ* toughened SiC have been reported elsewhere.[36]

The optimal mechanical properties, in terms of both high fracture toughness and strength, were achieved by hot-pressing at 1900°C, coinciding with conditions where the optimal microstructure was obtained. The physical and mechanical properties of the SiC hot-pressed at 1900°C for 1 h have been summarized in Table III.

IV. Conclusions

Hot-pressed SiC ceramics with Al, B, and C additives have been produced and evaluated. Through a liquid-phase sintering mechanism, dense SiC was obtained by hot-pressing at a temperature as low as 1700°C (with ≥3 wt% Al). In addition, the 3C (β) to 4H (α) phase transformation began at this temperature with 3wt%Al–0.6wt%B–2wt%C additions and completed at 1950°C. In association with the 3C-to-4H phase transformation, the SiC grains grew into platelike shapes. A thin (<1 nm) Al-containing amorphous grain boundary phase was detected by HR-TEM and was analyzed by AES. Grain bridging, pullout, and crack deflection accounted for an improvement in fracture toughness more than three times that of a commercial SiC. The *in situ* toughened SiC exhibited a significant rising *R*-curve behavior with a steady-state fracture toughness over 9 MPa·m$^{1/2}$, while retaining a high modulus of rupture of ~660 MPa.

Acknowledgment: We are grateful to Dr. B. J. Dalgleish for his assistance in sample preparations.

References

[1]G. Wei and P. Becher, "Improvements in Mechanical Properties in SiC by the Addition of TiC Particles," *J. Am. Ceram. Soc.*, **67** [8] 571–74 (1984).

[2]Y. Ohya, M. J. Hoffmann, and G. Petzon, "Sintering of *in-situ* Synthesized SiC-TiB_2 Composites with Improved Fracture Toughness," *J. Am. Ceram. Soc.*, **75** [9] 2479–83 (1992).

[3]T. Mitchell Jr., L. C. De Jonghe, W. J. MoberlyChan, and R. O. Ritchie, "Silicon Carbide Platelet/Silicon Carbide Composites," *J. Am. Ceram. Soc.*, **78** [1] 97–103 (1995).

[4]W. J. MoberlyChan, J. J. Cao, M. Y. Niu, and L. C. De Jonghe, "Toughened β-SiC Composites with Alumina-Coated α-SiC Platelets"; pp. 219–29 in *High Performance Composites—Commonalty of Phenomena*. Edited by K. K. Chawla, P. K. Liaw, and S. G. Fishman. TMS Publication, The Metallurgical Society, Warrendale, PA, 1994.

[5]J. J. Cao, W. J. MoberlyChan, L. C. De Jonghe, B. Dalgleish, and M. Y. Niu, "Processing and Characterization of SiC Platelet/SiC Composites"; pp. 277–88 in *Advances in Ceramic-Matrix Composites II*, Ceramic Transactions, Vol. 46. American Ceramic Society, Westerville, OH, 1995.

[6]K. Suzuki, "Pressureless-Sintered Silicon Carbide with Addition of Aluminum Oxide"; pp. 162–82 in *Silicon Carbide Ceramics—2*. Edited by S. Somiya and Y. Inomata. Elsevier Applied Science, New York, 1991.

[7]M. A. Mulla and V. D. Krstic, "Mechanical Properties of β-SiC Pressureless Sintered with Al_2O_3 Additions," *Acta Metall. Mater.*, **42** [1] 303–308 (1994).

[8]S. S. Shinozaki, J. Hangas, K. R. Carduner, M. J. Rokosz, K. Suzuki, and N. Shinohara, "Correlation between Microstructure and Mechanical Properties in Silicon Carbide with Alumina Addition," *J. Mater. Res.*, **8** [7] 1635–43 (1993).

[9]M. A. Mulla and V. D. Krstic, "Low-Temperature Pressureless Sintering of β-Silicon Carbide with Aluminum Oxide and Yttrium Oxide Additions," *Am. Ceram. Soc. Bull.*, **70** [3] 439–43 (1991).

[10]S. K. Lee and C. H. Kim, "Effects of α-SiC versus β-SiC Starting Powders on Microstructure and Fracture Toughness of SiC Sintered with Al_2O_3-Y_2O_3 Additives," *J. Am. Ceram. Soc.*, **77** [6] 1655–58 (1994).

[11]N. P. Padture, "*In Situ*-Toughened Silicon Carbide," *J. Am. Ceram. Soc.*, **77** [2] 519–23 (1994).

[12]N. P. Padture and B. R. Lawn, "Toughness Properties of a Silicon Carbide with an *in Situ* Induced Heterogeneous Grain Structure," *J. Am. Ceram. Soc.*, **77** [10] 2518–22 (1994).

[13]B. R. Lawn, *Fracture of Brittle Solids*, 2nd ed. Cambridge University Press, Cambridge, U.K., 1993.

[14]D. B. Marshall, "Controlled Flaws in Ceramics: A Comparison of Knoop and Vickers Indentation," *J. Am. Ceram. Soc.*, **66** [2] 127–31 (1983).

[15]P. Chantikul, G. R. Anstis, B. R. Lawn, and D. B. Marshall, "A Critical Evaluation of Indentation Techniques for Measuring Fracture Toughness: II, Strength Method," *J. Am. Ceram. Soc.*, **64** [9] 539–43 (1981).

[16]J. J. Petrovic and M. G. Mendiratta, "Fracture from Controlled Surface Flaw"; pp. 83–102 in *Fracture Mechanics Applied to Brittle Materials*, ASTM STP 678. Edited by S. W. Freiman. American Society for Testing and Materials, Philadelphia, PA, 1979.

[17]P. C. Paris, and G. C. Sih, "Stress Analysis of Cracks"; pp. 30–81 in *Fracture Toughness Testing and Its Applications*, ASTM STP. 381. American Society for Testing and Materials, Philadelphia, PA, 1965.

[18]R. H. Dauskardt and R. O. Ritchie, "Cyclic Fatigue–Crack Growth Behavior in Ceramics," *Closed Loop*, **17** [2] 7–17 (1989).

[19]R. H. Dauskardt, "A Frictional-Wear Mechanism for Fatigue-Crack Growth in Grain Bridging Ceramics," *Acta Metall. Mater.*, **41** [9] 2765–81 (1993).

[20]C. J. Gilbert, R. H. Dauskardt, R. W. Steinbrech, R. N. Petrany, and R. O. Ritchie, "Cyclic Fatigue in Monolithic Alumina: Mechanism of Crack Advance Promoted by Frictional Wear of Grain Bridges," *J. Mater. Sci.*, **30** [2] 643–54 (1995).

[21]J. Ruska, L. J. Gauckler, J. L. Lorenz, and H. U Rexer, "The Quantitative Calculation of SiC Polytypes from Measurements of X-ray Diffraction Peak Intensities," *J. Mater. Sci.*, **14** [8] 2013–17 (1979).

[22]R. Hamminger, G. Grathwohl, and F. Thummler, "Microanalytical Investigation of Sintered SiC," *J. Mater. Sci.*, **18** [2] 353–64 (1983).

[23]S. Shinozaki, J. Hangas, K. Maeda, and A. Soeta, "Enhanced Formation of 4H Polytype in Silicon Carbide Materials"; pp. 113–21 in *Silicon Carbide '87*, Ceramic Transactions, Vol. 2. Edited by J. D. Cawley and C. E. Semler. American Ceramic Society, Westerville, OH, 1987.

[24]S. Shinozaki, R. M. Williams, B. N. Juterbock, W. T. Donlon, J. Hangas, and C. R. Peters, "Microstructural Developments in Pressureless-Sintered β-SiC Materials with Al, B, and C Additions," *Am. Ceram. Soc. Bull.*, **64** [10] 1389–93 (1985).

[25]R. M. Williams, B. N. Juterbock, S. Shinozaki, C. R. Peters, and T. J. Whalen, "Effects of Sintering Temperatures on the Physical and Crystallographic Properties of β-SiC," *Am. Ceram. Soc. Bull.*, **64** [10] 1385–89 (1985).

[26]M. Srinivasan, "The Silicon Carbide Family of Structural Ceramics"; pp. 99–159 in *Structural Ceramics*, Treatise on Materials Science and Technology, Vol. 29. Edited by J. B. Wachtman Jr., Academic Press, New York, 1989.

[27]A. H. Heuer, G. A. Fryburg, L. U. Ogbuji, T. E. Mitchell, and S. Shinozaki, "β → α Transformation in Polycrystalline SiC: I, Microstructural Aspects," *J. Am. Ceram. Soc.*, **61** [9–10] 406–12 (1978).

[28]L. U. Ogbuji, T. E. Mitchell, and A. H. Heuer, "β → α Transformation in Polycrystalline SiC: III, Thickening of α Plates," *J. Am. Ceram. Soc.*, **64** [2] 91–99 (1981).

[29]R. A. Bishop and H. K. Bowen, "Suspension Processing of Beta-SiC Powders"; see Ref. 23, pp. 157–73.

[30]Y. Tajima and W. D. Kingery, "Solubility of Aluminum and Boron in Silicon Carbide," *J. Am. Ceram. Soc.*, **65** [2] C-27–C-29 (1982).

[31]Y. Inomata, H. Tanaka, Z. Inoue, and H. Kawabata, "Phase Relation in SiC–Al_4C_3–B_4C System at 1800°C," *J. Ceram. Soc. Jpn.*, **88** [6] 353–55 (1980).

[32]L. M. Foster, G. Long, and M. S. Hunter, "Reactions between Aluminum Oxide and Carbon," *J. Am. Ceram. Soc.*, **39** [1] 1–11 (1956).

[33]I. Merkel and U. Messerschmidt, "Fracture Toughness of Sintered SiC Ceramics: A Comparison between Different Methods," *Mater. Sci. Eng., A*, **151** [2] 131–35 (1992).

[34]P. F. Becher, "Microstructural Design of Toughened Ceramics," *J. Am. Ceram. Soc.*, **74** [2] 255–69 (1991).

[35]K. T. Faber and A. G. Evans, "Crack Deflection Processes—I. Theory," *Acta Metall.*, **31** [4] 565–76 (1983).

[36]C. J. Gilbert, J. J. Cao, W. J. MoberlyChan, L. C. De Jonghe, and R. O. Ritchie, "Cyclic Fatigue and Resistance-Curve Behavior of an *in Situ* Toughened Silicon Carbide with Al-B-C Additions," *Acta Metall. Mater.*, in press, 1995. □